UC San Diego

UC San Diego Previously Published Works

Title

Microtubules and actin microfilaments regulate lipid raft/caveolae localization of adenylyl cyclase signaling components

Permalink

https://escholarship.org/uc/item/3mg4q2fb

Journal

The Journal of biological chemistry, 281(36)

ISSN

0021-9258

Authors

Head, Brian P
Patel, Hemal H
Roth, David M
et al.

Publication Date

2006-09-08

Peer reviewed

eScholarship.org Powered by the California Digital Library
University of California

THE JOURNAL OF BIOLOGICAL CHEMISTRY VOL. 281, NO. 36, pp. 26391–26399, September 8, 2006
Printed in the U.S.A.

Microtubules and Actin Microfilaments Regulate Lipid Raft/Caveolae Localization of Adenylyl Cyclase Signaling Components*

Received for publication, March 20, 2006, and in revised form, June 16, 2006 Published, JBC Papers in Press, July 3, 2006, DOI 10.1074/jbc.M602577200

Brian P. Head[‡], Hemal H. Patel[‡§], David M. Roth[§¶], Fiona Murray[‡], James S. Swaney[‡], Ingrid R. Niesman[‖], Marilyn G. Farquhar[‖], and Paul A. Insel[‡1]**

*From the [‡]Departments of Pharmacology, [§]Anesthesiology, [‖]Cellular and Molecular Medicine, and **Medicine, University of California, San Diego, La Jolla, California 92093 and [¶]Veterans Affairs San Diego Healthcare System, San Diego, California 92161*

Microtubules and actin filaments regulate plasma membrane topography, but their role in compartmentation of caveolae-resident signaling components, in particular G protein-coupled receptors (GPCR) and their stimulation of cAMP production, has not been defined. We hypothesized that the microtubular and actin cytoskeletons influence the expression and function of lipid rafts/caveolae, thereby regulating the distribution of GPCR signaling components that promote cAMP formation. Depolymerization of microtubules with colchicine (Colch) or actin microfilaments with cytochalasin D (CD) dramatically reduced the amount of caveolin-3 in buoyant (sucrose density) fractions of adult rat cardiac myocytes. Colch or CD treatment led to the exclusion of caveolin-1, caveolin-2, β_1-adrenergic receptors (β_1-AR), β_2-AR, $G\alpha_s$, and adenylyl cyclase $(AC)_{5/6}$ from buoyant fractions, decreasing $AC_{5/6}$ and tyrosine-phosphorylated caveolin-1 in caveolin-1 immunoprecipitates but in parallel increased isoproterenol (β-AR agonist)-stimulated cAMP production. Incubation with Colch decreased co-localization (by immunofluorescence microscopy) of caveolin-3 and α-tubulin; both Colch and CD decreased co-localization of caveolin-3 and filamin (an F-actin cross-linking protein), decreased phosphorylation of caveolin-1, Src, and p38 MAPK, and reduced the number of caveolae/μm of sarcolemma (determined by electron microscopy). Treatment of S49 T-lymphoma cells (which possess lipid rafts but lack caveolae) with CD or Colch redistributed a lipid raft marker (linker for activation of T cells (LAT)) and $G\alpha_s$ from lipid raft domains. We conclude that microtubules and actin filaments restrict cAMP formation by regulating the localization and interaction of GPCR-G_s-AC in lipid rafts/caveolae.

The three components of the cytoskeleton, intermediate filaments, microtubules, and actin filaments (microfilaments), contribute to the structural organization of the cytoplasm and help regulate the topography of the plasma membrane in eukaryotic cells (1–3). Microtubules and actin filaments have nucleotide binding and hydrolyzing activity, whereas intermediate filaments, which serve as cytoskeletal "identity cards" that distinguish different cell types, have no known enzymatic activity. Disassembly of the actin filament cytoskeleton, which is involved in cell motility, adhesion, and endocytosis, leads to fusion of intracellular vesicular membranes with the plasma membrane (4). Microtubules, the polymerized tubulin cytoskeleton, are involved in cell locomotion, movement of organelles, and mitosis. Both actin filaments and microtubules are implicated in membrane trafficking in mitotic cells (5). Moreover, considerable work over the past 30 years has documented that cytoskeletal disrupting agents, in particular inhibitors of microtubules and actin filaments, can enhance signaling by G protein-coupled receptors (GPCR),[2] in particular GPCR that are linked to the activation of adenylyl cyclase (AC) and increased cAMP synthesis (6–9). The molecular basis for this action is unknown.

Recent data implicate a connection between cytoskeletal components and caveolar-regulated cellular events (4, 5, 10). Caveolae, 50–100-nm invaginations of the plasma membrane that contain cholesterol, sphingolipids, and the structural protein caveolin (which exists in 3 isoforms, caveolins-1, -2, and -3 (11, 12)) can serve as sites for actin "tail" formation (4) and can be anchored to the cell surface by cortical actin filaments (13). Caveolae participate in diverse functions, including endocytosis (14), calcium homeostasis (15), skeletal muscle transverse tubule formation (16), and compartmentation of receptor-mediated signaling components (17, 18). Among the latter are GPCR, heterotrimeric G proteins, and GPCR/G protein-regulated effector molecules, a population of which localize in caveolae, thereby facilitating coordinated and rapid generation of second messengers and regulation of cell function (17, 18). However, the contribution of microtubules and actin filaments to caveolae-regulated signal transduction, in particular GPCR-G_s-protein-AC-cAMP signaling, is unknown.

* This work was supported by National Institutes of Health Grants GM66232 and HL66941. The costs of publication of this article were defrayed in part by the payment of page charges. This article must therefore be hereby marked "*advertisement*" in accordance with 18 U.S.C. Section 1734 solely to indicate this fact.

[1] To whom correspondence should be addressed: University of California, San Diego, Dept. of Pharmacology, 9500 Gilman Dr., BSB 3076 La Jolla, CA 92093-0636. Tel.: 858-534-2295; Fax: 858-822-1007; E-mail: pinsel@ucsd.edu.

[2] The abbreviations used are: GPCR, G protein-coupled receptor; AC, adenylyl cyclase; β-AR, β-adrenergic receptor; BF, buoyant fraction; CM, cardiac myocyte; Cav, caveolin; P-Cav, phosphorylated Cav; Colch, colchicine; CD, cytochalasin D; HF, heavy fraction; LAT, linker of activated T cell; P-p38, phosphorylated p38 mitogen-activated protein kinase (MAPK); P-Src, phosphorylated Src tyrosine kinase; PBS, phosphate-buffered saline; MES, 4-morpholineethanesulfonic acid.

Downloaded from www.jbc.org at Biomedical Library, UCSD on April 15, 2009

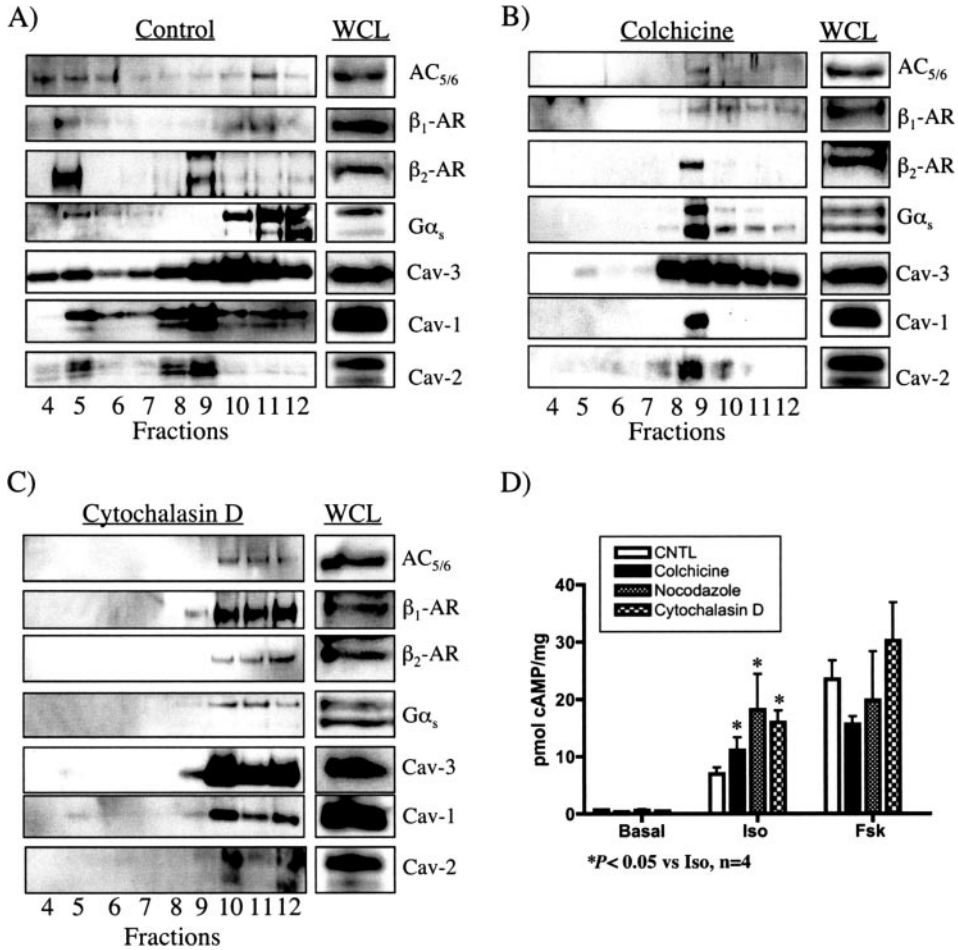

FIGURE 1. **Distribution of $AC_{5/6}$, β_1-AR, β_2-AR, $G\alpha_s$, and caveolin (*Cav*) isoforms and effects on isoproterenol-stimulated cAMP accumulation after cytoskeletal disruption of adult CMs.** *A*, $AC_{5/6}$, β_1-AR, β_2-AR, $G\alpha_s$, Cav-1, -2, and -3 were detected in BF (*lanes 4* and *5*) and HF (*lanes 10–12*) from sucrose density fractionation of Na_2CO_3 extracts. Colch (30 μM; 1 h) (*B*) and CD (20 μM; 1.5 h) (*C*) treatment of adult CM resulted in the exclusion of $AC_{5/6}$, β_1-AR, β_2-AR, $G\alpha_s$, Cav-1, -2, and -3 from BF without changing total cellular protein levels as indicated in whole cell lysates (*WCL*). *D*, isoproterenol (*iso*, 10 min)-, but not forskolin (*Fsk*, 10 min)-stimulated cAMP accumulation significantly increased ($p < 0.05$) in CMs treated with Colch, nocodazole (*Nocod*, 33 μM; 1 h), and CD compared with non-treated CM. Data are expressed as total pmol of cAMP/mg ± S.E. (63,000 cells/well), conducted in triplicate from cell isolated from four different animals ($n = 4$). *CNTL*, control.

An example of a physiologically important GPCR is the β-adrenergic receptor (β-AR), whose activation by the sympathetic nervous system or circulating catecholamines is a key mechanism for the production of cAMP in numerous tissues, including the mammalian heart (19). As indicated above, substantial data indicate that β-AR-stimulated cAMP formation can be enhanced by agents that disrupt microtubules or actin filaments, but the precise mechanisms have not been defined (6, 20, 21). Other findings indicate co-localization with and regulation by caveolins of β-AR and other GPCR, G_s, and ACs (18, 22). Because the effectiveness of this signaling cascade depends upon the organization and location of signaling proteins within the plasma membrane, we tested for a mechanistic link between the localization of GPCR signaling components in caveolae and the ability of cytoskeletal agents to alter β-AR signal transduction. We, thus, assessed the impact of disruption of microtubules and actin filaments on the distribution of caveolae, caveolins, and GPCR signaling components as related to GPCR-G_s mediated-cAMP production. The results indicate that intact microtubules and actin filaments contribute to the presence of caveolae and tonic inhibition of GPCR-G_s-AC signal transduction.

EXPERIMENTAL PROCEDURES

Materials—Antibodies were: to $AC_{5/6}$, β_1-AR, β_2-AR, and $G\alpha_s$ (Santa Cruz Biotechnology, Santa Cruz, CA); to caveolin-3, caveolin-2, caveolin-1 (monoclonal), and phosphorylated caveolin (P-Cav) (BD Biosciences); to caveolin-3 (polyclonal) and to linker for activation of T cells (LAT) (AbCam, Cambridge, MA); to Src, P-Src, p38, and P-p38 kinase antibodies (Cell Signaling, Beverly, MA); to phosphorylated extracellular signal-regulated kinase 1/2 (Stressgen, Victoria, BC, Canada). Glyceraldehyde-3-phosphate dehydrogenase antibody was obtained from Imgenex (San Diego, CA). Fluorescein isothiocyanate and Alexa-conjugated secondary antibodies were from Molecular Probes (Carlsbad, CA)/Invitrogen. Other secondary antibodies were obtained from Santa Cruz Biotechnology. Filamin and α-tubulin and all other chemicals and reagents were obtained from Sigma unless otherwise stated.

Culture of Cardiac Myocytes (CMs) and S49 Cells—Adult male Sprague-Dawley rats (250–300 g) or C57BL mice (aged 8–10 weeks, 24–26 g) or Cav-$1^{-/-}$ mice (The Jackson Laboratory Bar Harbor, Maine) were anesthetized with ketamine (100 mg/kg) and xylazine (10 mg/kg), and hearts were excised and retrograde-perfused with media containing collagenase II, as previously described (18). Animals were heparinized (1000–2000 units intraperitoneally) 5 min before anesthesia. Hearts were removed, placed in ice-cold cardioplegic solution (containing in 112 mM NaCl, 5.4 mM KCl, 1 mM $MgCl_2$, 9 mM NaH_2PO_4, 11.1 mM D-glucose, 10 mM Hepes, 30 mM taurine, 2 mM DL-carnitine, 2 mM creatine, pH 7.4) and retrograde-perfused on a Langendorff apparatus for 5 min at 5 ml/min at 37 °C and then for 20 min with media containing collagenase II (250 units/mg; Worthington). Ventricles were minced in collagenase II-containing media for 10–15 min, washed several times, and placed in 1.2 mM Ca^{2+} for 25 min to produce calcium-tolerant CMs. CMs were plated in 4% fetal bovine serum on laminin (2 $\mu g/cm^2$)-coated plates for 1 h and then serum-free medium (1% bovine serum albumin) to remove non-myocytes. CMs were incubated at 37 °C in 5% CO_2 for 24 h before experiments. S49 cells were grown in Dulbecco's modified Eagle's medium supplemented with 10% heat-inactivated horse serum

Downloaded from www.jbc.org at Biomedical Library, UCSD on April 15, 2009

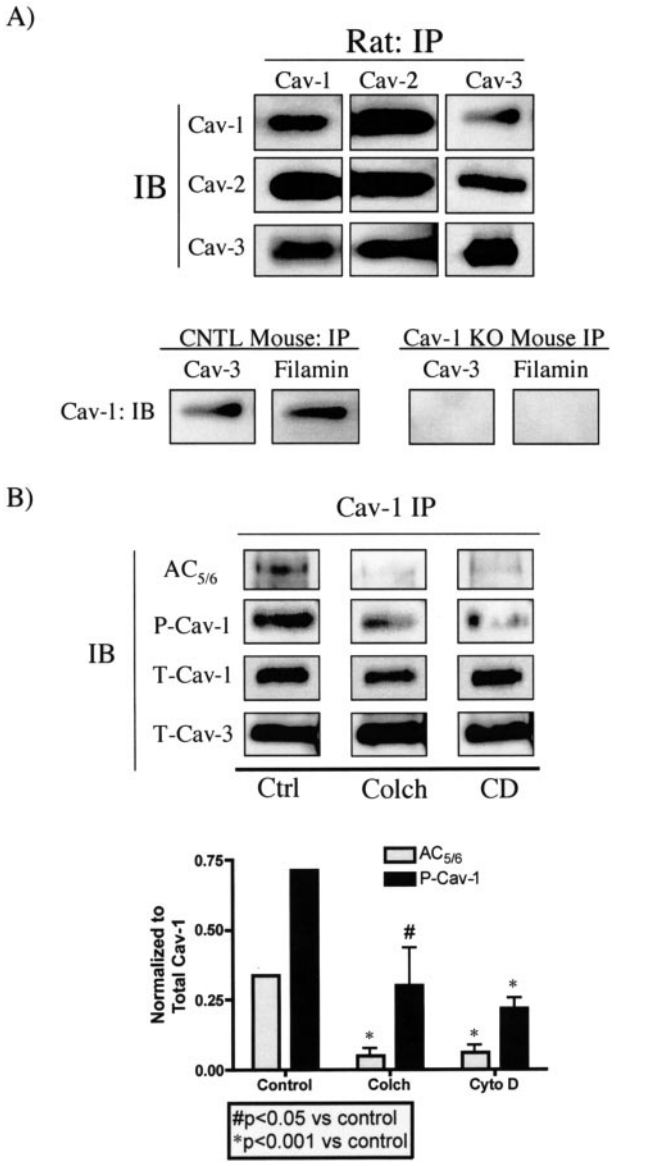

FIGURE 2. **Caveolin isoforms co-immunoprecipitate in adult CM lysates.** *A*, immunoblot (*IB*) analysis shows Cav-1, -2, and -3 in Cav-1, -2, and -3 immunoprecipitates (*IP*) of adult CMs. Caveolin-1 was detected in caveolin-3 and filamin immunoprecipitates of wild-type CMs but not in caveolin-3 and filamin immunoprecipitates from caveolin-1 null adult CM. *B*, $AC_{5/6}$, P-Cav-1, Cav-1, and Cav-3 were detected in Cav-1 immunoprecipitates of CM lysates. Treatment with Colch and CD (*Cyto D*) significantly ($p < 0.05$; experiments conducted on cells from 3 separate animals) decreased the detection of $AC_{5/6}$ and P-Cav-1 in caveolin-1 immunoprecipitates. *CNTL*, control.

and 10 μM HEPES in 10% CO_2 at 37 °C; S49 cells were studied at 10^6 cells/ml.

Membrane Fractionation—CM and S49 cells were fractionated using a detergent-free method (23). CM from a 15-cm plate or 10^7 S49 cells were washed twice in ice-cold PBS and scraped in 3 ml of either 500 mM Na_2CO_3, pH 11.0, to extract peripheral membrane proteins. Cells were homogenized using three 10-s bursts of a tissue grinder and then sonicated with 3 cycles of 20-s bursts of sonication and a 1-min incubation on ice. Approximately 2 ml of homogenate were mixed with 2 ml of 90% sucrose in 25 mM MES, 150 mM NaCl (MBS, pH 6.5) to form 45% sucrose and loaded at the bottom of an ultracentrifuge tube. A discontinuous sucrose gradient was generated by layering 4 ml of 35% sucrose prepared in MBS, 250 mM Na_2CO_3 followed by 4 ml of 5% sucrose (in MBS/Na_2CO_3). Gradients were centrifuged at 280,000 × *g* using a SW41Ti rotor (Beckman) for 16–20 h at 4 °C. Samples were removed in 1-ml aliquots to form 12 fractions.

Immunoprecipitation—Immunoprecipitations were performed using either protein A or protein G-agarose (Roche Applied Science). Lysates were incubated with primary antibody for 1–3 h at 4 °C, immunoprecipitated with protein-agarose overnight at 4 °C, and then spun for 5 min at 13,000 × *g*. The pellets were washed in lysis buffer (50 mM Tris-HCl, pH 7.5, 500 mM NaCl, 1% IGEPAL CA-630) then in wash buffer 2 (50 mM Tris-HCl, pH 7.5, 500 mM NaCl, 0.2% IGEPAL CA-630) and wash buffer 3 (10 mM Tris-HCl, pH 7.5, 0.2% IGEPAL CA-630).

Immunoblot Analysis—Proteins were separated by SDS-PAGE using 10 or 12% acrylamide gels (Invitrogen) and transferred to polyvinylidene difluoride membranes (Millipore) by electroelution. Membranes were blocked in 20 mM PBS Tween (1%) containing 1.5% nonfat dry milk and incubated with primary antibody overnight at 4 °C. Primary antibodies were visualized using secondary antibodies conjugated with horseradish peroxidase (Santa Cruz Biotechnology) and ECL reagent (Amersham Biosciences). All displayed bands migrated at the appropriate size as compared with molecular weight standards (Santa Cruz Biotechnology). The amount of protein per fraction was determined using a dye-binding protein assay (Bio-Rad).

Immunofluorescence Microscopy of CMs—CMs were prepared for immunofluorescence microscopy as described (18) with growth for 24 h after plating on precoated laminin (2 $\mu g/cm^2$) glass coverslips. Cells were fixed with 2% paraformaldehyde in PBS for 10 min at room temperature, incubated with 100 mM glycine, pH 7.4, for 10 min to quench aldehyde groups, permeabilized in buffered Triton X-100 (0.1%) for 10 min, blocked with 1% bovine serum albumin (BSA), PBS, Tween (0.05%) for 20 min, and then incubated with primary antibodies (1:100) in 1% BSA, PBS, Tween (0.05%) for 24–48 h at 4 °C. Excess antibody was removed by incubation with PBS, Tween (0.1%) for 15 min; samples were then incubated with fluorescein isothiocyanate or Alexa-conjugated secondary antibody (1:250) for 1 h. To remove excess secondary antibody, cells were washed 6× at 5-min intervals with PBS, Tween (0.1%) and incubated for 20 min with the nuclear stain 4′,6-diamidino-2-phenylindole (1:5000) diluted in PBS. Cells were washed for 10 min with PBS and mounted in gelvatol for microscopic imaging.

Deconvolution Image Analysis—Deconvolution images were obtained (18) and captured with a DeltaVision deconvolution microscope system (Applied Precision, Inc., Issaquah, WA), which includes a Photometrics CCD mounted on a Nikon TE-200 inverted epifluorescence microscope. Between 30 and 80 optical sections spaced by ~0.1–0.3 μm were taken. Exposure times were set so that the camera response was in the linear range for each fluorophore. Data sets were deconvolved and analyzed using SoftWorx software (Applied Precision, Inc.) on a Silicon Graphics Octane work station. Image analysis was performed with the Data Inspector program in SoftWorx. Maximal projection volume views or single optical sections are shown as indicated.

Downloaded from www.jbc.org at Biomedical Library, UCSD on April 15, 2009

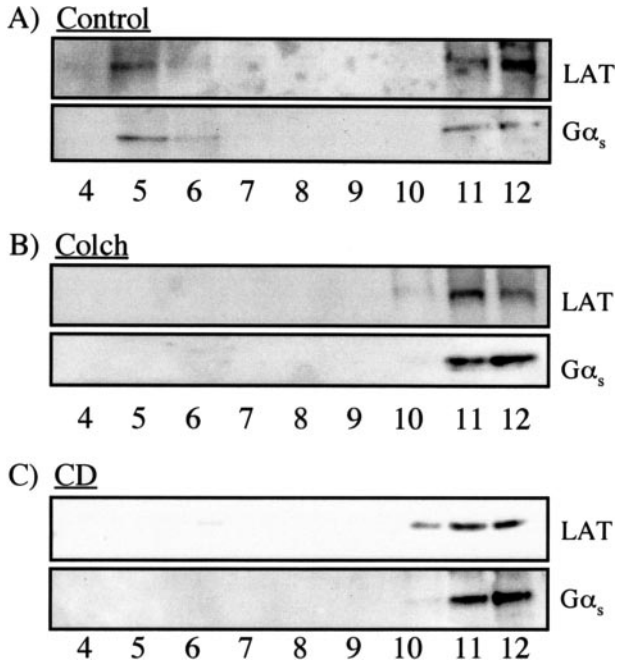

FIGURE 3. **Distribution of LAT and $G\alpha_s$ after treatment of S49 cells with colchicine and cytochalasin D.** *A*, LAT and $G\alpha_s$ were detected in BF (*lanes 4* and *5*) and HF (*lanes 10–12*) from sucrose density fractionation after Na_2CO_3 extraction. *B*, Colch (30 μM; 1 h) and CD (20 μM; 1.5 h) (*C*) treatment resulted in the total exclusion of LAT and $G\alpha_s$ from BF. Similar data were obtained in three separate experiments.

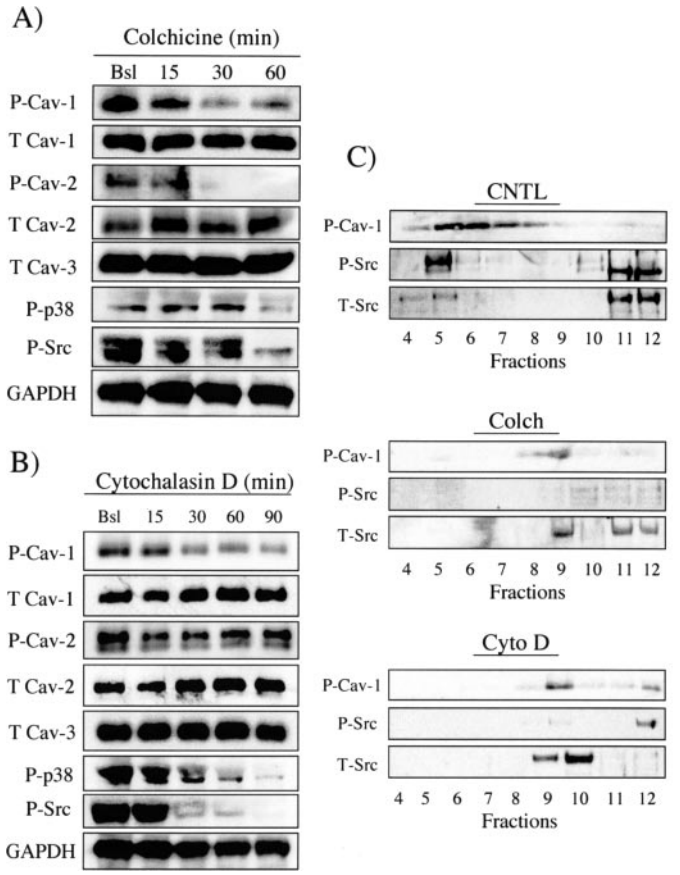

FIGURE 4. **Cytoskeletal disruption of adult cardiac myocytes decreases phosphorylation of caveolins, p38 MAPK, and Src tyrosine kinase.** CMs were treated with Colch (30 μM) for 15, 30, and 60 min or CD (20 μM) for 15, 30, 60, and 90 min followed by immunoblot analysis. *GAPDH*, glyceraldehyde-3-phosphate dehydrogenase. *A*, Colch treatment decreased the amount of P-Cav-1, P-Cav-2, P-p38 MAPK, and P-Src tyrosine kinase after 60 min, whereas total Cav-1, Cav-2, and Cav-3 protein expression did not change. *B*, CD treatment decreased P-Cav-1, P-p38, and P-Src after 90 min without altering protein expression of total Cav-1, Cav-2, and Cav-3. *C*, P-Cav-1, P-Src, Total Src tyrosine kinase redistributed to HF after Colch and CD (*Cyto D*) treatment. *CNTL*, control.

Quantitation of Co-localization—We quantitated the co-localization of pixels using CoLocalizer Pro 1.0 software. Overlap coefficient according to Manders (MOC) was used to determine the degree of colocalization on whole cells or sarcolemmal regions after subtracting background through normalized threshold values (24). The values are defined by 0–1 (1 implying that 100% of both components overlap with the other part of the image). Statistics were performed with Prism.

Electron Microscopy—Cells were fixed with 2.5% glutaraldehyde in 0.1 M cacodylate buffer for 2 h at room temperature, postfixed in 1% OsO_4 in 0.1 M cacodylate buffer (1 h) at room temperature, and embedded as monolayers in LX-112 (Ladd Research, Williston, VT), as described previously (25). Sections were stained in uranyl acetate and lead citrate and observed with the use of an electron microscope (JEOL 1200 EX-II or Philips CM-10). Caveolae were identified as 50–100-nm invaginations or vesicles within several nanometers of the membrane and quantitated on random images per length of membrane.

Measurement of cAMP Production—We assayed cAMP accumulation by incubating cells for 10 min with drugs of interest and 0.2 mM isobutylmethylxanthine, a cyclic nucleotide phosphodiesterase inhibitor. To terminate the reaction, assay medium was aspirated, and 250 μl of ice-cold trichloroacetic acid (7.5%, w/v) was added. cAMP content in trichloroacetic acid extracts was determined by radioimmunoassay (18). Production of cAMP was normalized to the amount of protein per sample (63,000 cells/well) as determined using a dye-binding protein assay (Bio-Rad).

Statistical Analysis—Data are expressed as mean ± S.E. Student's unpaired *t* test was used to compare treatment groups with significance established at a level of $p < 0.05$.

RESULTS

Caveolin Isoforms, β-AR, $G\alpha_s$, and $AC_{5/6}$ Are Excluded from Buoyant Fractions of Adult CM after Cytoskeletal Disruption—To test the impact of cytoskeletal disrupting agents on expression and co-localization of caveolins and GPCR-G_s-AC, we investigated the distribution of caveolin-3 and signaling components in fractions prepared by sucrose density gradient fractionation of adult CMs treated with Colch or CDs using conditions previously validated to lead to inhibition of microtubule and actin filament assembly, respectively (26–28). Treatment with Colch or CD redistributed caveolins 1, 2, and 3 from buoyant fractions (fractions 4 and 5, termed buoyant caveolin-rich fractions (BF)) to heavy/non-buoyant fractions (fractions 9–12 (HF)) and similarly redistributed β_1-AR, β_2-AR, $AC_{5/6}$, and $G\alpha_s$ (Fig. 1*A–C*) without changing protein expression in Colch- and CD-treated whole cell lysates (*WCL*) compared with control. In parallel with the redistribution of signaling components, the β-AR agonist isoproterenol stimulated the generation of more cAMP in Colch-, nocodazole (another microtubule disrupter)-, and CD-treated CMs (Fig. 1*D*; $p < 0.05$ *versus* control). These results show that agents that depo-

Downloaded from www.jbc.org at Biomedical Library, UCSD on April 15, 2009

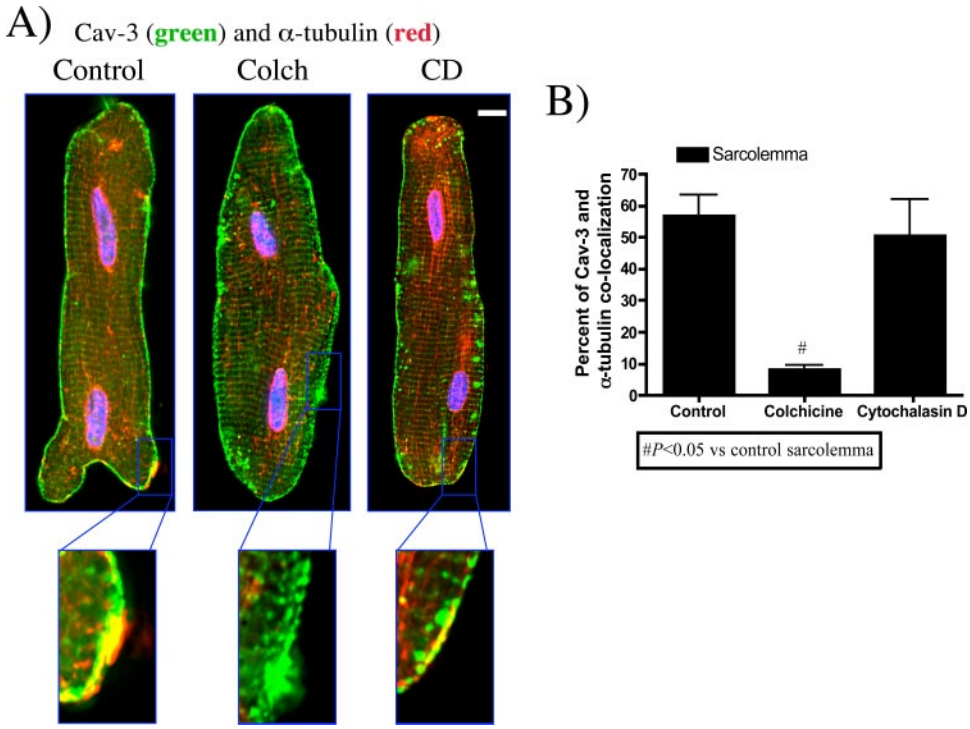

FIGURE 5. **Immunofluorescence and de-convolution analysis of the co-localization between caveolin-3 and the microtubule marker (α-tubulin) after cytoskeletal disruption of adult cardiac myocytes.** *A*, immunofluorescence microscopy reveals that sarcolemmal co-localization between caveolin-3 and α-tubulin is significantly decreased ($p < 0.05$ *versus* control, 3–5 cells from 3 separate experiments) after Colch (30 μM) treatment. *B*, data from *panel B* is expressed as the percent co-localization between caveolin-3 and α-tubulin on the sarcolemmal membrane. Images were de-convolved and shown as single-stained or overlaid to show co-localization. *Scale bar*, 10 μm.

lymerize microtubules and actin filaments redistribute caveolin isoforms and β-AR signaling components (*i.e.* β-ARs, $AC_{5/6}$, $G\alpha_s$) from BF to HF and enhance β-AR-stimulated cAMP production, indicating that despite cellular redistribution of caveolins and disruption of caveolae (corroborated by electron microscopy, to be shown subsequently (see Fig. 6)) components involved in cAMP generation have more catalytically productive interactions.

Co-immunoprecipitation Reveals Caveolin-1 and Caveolin-3 in Multiprotein Complexes in CMs—As suggested by previous work (29) regarding the interaction of caveolins and formation of hetero-oligomeric complexes, caveolin 1, 2, and 3 co-immunoprecipitated in lysates of CMs (Fig. 2*A*). Filamin is an F-actin cross-linking protein that can interact with caveolin-1 (10, 30). To test whether such an interaction occurs in CM, we assessed whether caveolin-1 and caveolin-3 are present in filamin immunoprecipitates from CMs prepared from wild-type and caveolin-1 null mice; we detected caveolin-1 in both caveolin-3 and filamin immunoprecipitates prepared from control but not caveolin-1-null mice (Fig. 2*A*). Colch and CD decreased detection of $AC_{5/6}$ and phosphorylated caveolin-1 in caveolin-1 immunoprecipitates from adult CM (Fig. 2*B*). Thus, all three caveolin isoforms are expressed and form multiprotein complexes in adult CM lysates, and inhibition of either microtubules or actin filaments decreases detection of phosphorylated caveolin-1 and AC in caveolin-associated complexes.

Colch and CD Treatment Redistributes Linker for Activation of T Cells (LAT) and $G\alpha_s$ from Buoyant Fractions in S49 Cells—Previous work has demonstrated that treatment of murine S49 T-lymphoma cells with Colch and CD enhances β-AR-mediated cAMP production by post-β-AR actions (8). S49 cells possess lipid rafts but lack caveolae (32, 33). LAT is an integral membrane protein and a marker for lipid rafts in T cells; lipid rafts can be isolated in buoyant fractions of disrupted cells (34, 35). $G\alpha_s$ has also been identified as a lipid raft constituent in T cells (34, 35). We, thus, used murine S49 T-lymphoma cells to assess the impact of Colch and CD on localization of these lipid raft signaling components. We found that LAT and $G\alpha_s$ of S49 cells partially localize in buoyant fractions after sucrose density fractionation (Fig. 3*A*). Treatment with Colch (Fig. 3*B*) and CD (Fig. 3*C*) redistributed LAT and $G\alpha_s$ to heavy fractions. Thus, disruption of microtubules and actin microfilaments redistributes components involved in cAMP production and T cell activation from lipid raft fractions in S49 cells.

Treatment with Colch and CD Decreases Caveolin-1, p38 MAPK, and Src Phosphorylation in Adult CMs—In further studies with adult CMs we assessed signaling components that are distal to the generation of cAMP and also examined the impact of cytoskeletal disruptors on the expression of tyrosine-phosphorylated caveolin-1 and -2 (P-Cav-1 and -2), whose phosphorylation is mediated by Src tyrosine kinase family members (34). Colch treatment decreased the amount of P-Cav-1, P-Cav-2, P-p38, and P-Src, albeit the latter exhibited a somewhat slower time course (Fig. 4*A*). CD treatment decreased expression of P-Cav-1, P-p38, and P-Src but not P-Cav-2 (Fig. 4*B*). Phosphorylated extracellular signal-regulated kinase 1/2 expression was not altered after treatment with Colch or CD (data not shown). Sucrose density centrifugation revealed that in control cells the majority of P-Cav-1 and P-Src (but not Src (T-Src in Fig. 4*C*)) distribute to BF, with some P-Src in HF; Colch or CD treatment decreased and redistributed P-Cav-1, P-Src, and T Src (Fig. 4*C*). The antibody for P-Src may cross-react with other Src family members in equivalent phosphorylation states (according to the antibody manufacturer), thus potentially explaining the different bands detected in BF and HF. Overall, these studies demonstrate that disruption of microtubules and actin filaments in adult CM alters phosphorylation of caveolin (without changing total caveolin expression), p38, and Src.

Immunofluorescence Microscopy of Adult CMs after Treatment with Colch and CD Reveals Irregular Caveolin-3 Clusters in Subsarcolemmal Regions—We used immunofluorescence microscopy to directly assess the intracellular distribution of caveolin-3 after cytoskeletal disruption. In untreated cells, caveolin-3 co-localized with α-tubulin on the sarcolemma (Fig. 5*A*, *left image*).

Downloaded from www.jbc.org at Biomedical Library, UCSD on April 15, 2009

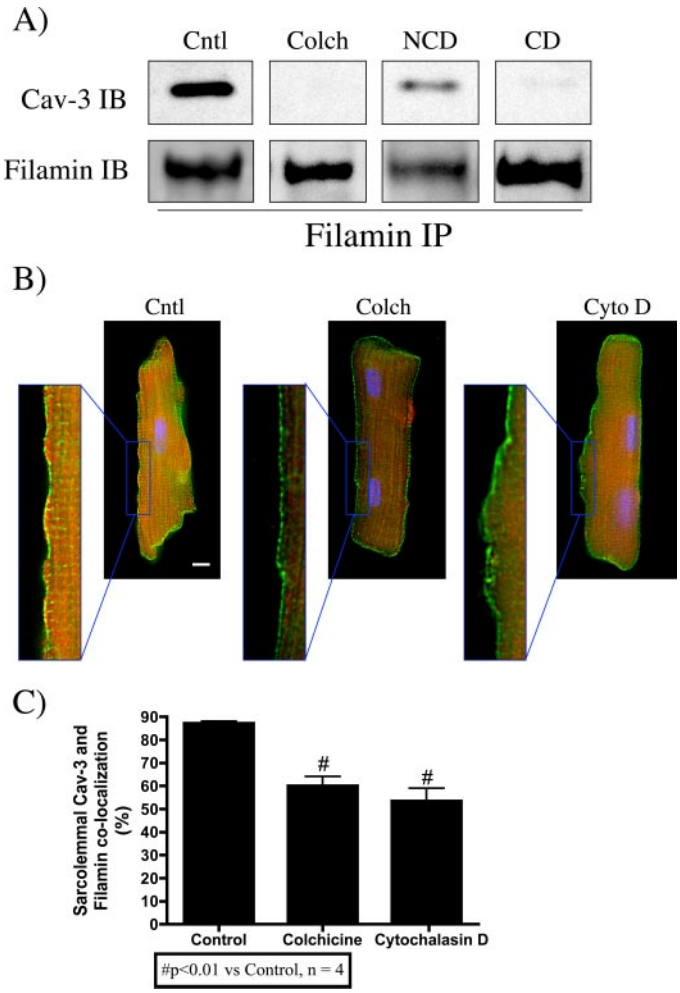

FIGURE 6. **Cytoskeletal disruption decreases co-localization between caveolin-3 and filamin in cardiac myocytes.** *A*, caveolin-3 was detected in filamin immunoprecipitates of CM lysates. Treatment with Colch (*Colc*, 30 μM; 1 h), CD (*Cyto D*, 20 μM; 1.5 h), and nocodazole (*NCD*, 33 μM; 1 h) decreased the amount of caveolin-3 detected in filamin immunoprecipitates. *Ctrl*, control. *B*, co-localization of caveolin-3 with filamin on the sarcolemmal membrane was significantly reduced ($p < 0.01$) in the presence of Colch and CD, as indicated by a reduction in yellow fluorescence (overlapping pixels). *C*, data from Fig. 6*B* are expressed as percent sarcolemma co-localization between caveolin-3 and filamin and was quantitated on 3–5 cells from 4 separate experiments. Images were de-convolved and shown as single-stained or overlaid to show co-localization. *Scale bar*, 10 μm.

Colch treatment decreased co-localization between caveolin-3 and α-tubulin in the sarcolemma ($p < 0.05$ *versus* control) (Fig. 5*B*). Treatment with CD resulted in irregular caveolin-3 clusters in subsarcolemmal regions; quantitation revealed no reduction in co-localization between caveolin-3 and α-tubulin, in particular on the sarcolemma. Thus, co-localization between caveolin-3 and α-tubulin depends upon proper assembly of microtubules, with cytoskeletal disruption leading to irregular clustering of caveolin-3 in subsarcolemmal and intracellular regions.

Co-localization of Caveolin-3 and Filamin Is Decreased after Cytoskeletal Disruption—To determine whether filamin, an F-actin cross-linking protein and ligand of caveolin-1 (10), is detected in multiprotein complexes with caveolin-3, we performed immunoprecipitation with CM lysates using a filamin antibody; we detected caveolin-3 in filamin immunoprecipitates (Fig. 6*A*). Treatment with Colch, nocodazole, and CD decreased the amount of caveolin-3 in filamin immunoprecipitates. Immunofluorescence microscopy demonstrated co-localization of caveolin-3 and filamin on the sarcolemmal membrane and in subsarcolemmal regions but decreased co-localization after disruption of microtubules or actin filaments (Fig. 6, *B* and *C*). Thus, caveolin-3 localizes in multiprotein complexes with filamin; this complex is disrupted after depolymerization of microtubules or actin filaments.

Immunofluorescence Microscopy of Cytoskeletal-disrupted Adult CMs Reveals a Significant Reduction in Phosphorylation of Caveolin-1—Treatment of CM with either Colch or CD decreased expression of P-Cav-1, as determined by immunoblotting (Fig. 2) and fractionation (Fig. 4), but also altered cellular expression and distribution, as assessed by immunofluorescence microscopy (Fig. 7). Control CM incubated with antibodies for P-Cav-1 (*red pixels*) and Cav-3 (*green pixels*) revealed discrete regions of co-localization on the sarcolemmal membrane and in sparse regions within the cell interior (Fig. 7*A*, *far left image*). Treatment with Colch or CD reduced caveolin-1 phosphorylation ($p < 0.0001$ *versus* control, Fig. 7, *A* and *B*). Thus, both immunoblotting (Figs. 2 and 4) and microscopy (Fig. 7) reveal that cytoskeletal disruption decreases P-Cav-1 in adult CMs.

Cytoskeletal Disruption Decreases the Number of Caveolae in CMs—We used electron microscopy to assess the presence of caveolae (50–100-nm membrane invaginations or vesicles within close proximity (~5–10 nm) to the sarcolemma) and observed loss of caveolae after Colch or CD treatment (Fig. 8). Control CMs had abundant caveolae along the sarcolemma closely apposed to subsarcolemmal mitochondria (within 0.5 μm of sarcolemma) (Fig. 8*A*), but treatment with Colch (Fig. 8*B*) or CD (Fig. 8*C*) decreased the expression of caveolae on the sarcolemma (Fig. 8, *Bi* and *Ci*) and near subsarcolemmal mitochondria (Fig. 8, *Bii* and *Cii*). Incubation with Colch resulted in vacuoles associated with Ω-shaped membranes similar to caveolae (Fig. 8*Biii*), whereas treatment with CD yielded 50–100-nm diameter structures adjacent to the sarcolemma resembling fused caveolae (Fig. 8*Ciii*). Colch or CD treatment decreased the number of caveolae ~60% (Fig. 8*D*).

DISCUSSION

Microtubules and the actin-associated cytoskeleton (*i.e.* actin filaments) are key cellular components for establishing membrane topography, trafficking, and organelle movement. Function of cellular membranes (*e.g.* signal transduction) can be regulated by microtubules and the actin cytoskeleton (6, 9, 20, 21), and the role of those cytoskeletal components changes during age and disease (35). We combined the use of biochemical and microscopic techniques to investigate the role of microtubules and actin filaments in the expression of caveolae and the compartmentation of β-AR-G_s-AC signaling components. We focused our efforts on adult CMs because 1) β-AR-G_s-AC signaling components localize in caveolin-associated microdomains in these cells (18), 2) alterations in microtubule content (35, 36) (despite the low abundance of cardiomyocyte tubulin (~0.01% of myocyte protein)) and changes in number and morphology of caveolae occur during cardiac hypertrophy (37), and 3)

Downloaded from www.jbc.org at Biomedical Library, UCSD on April 15, 2009

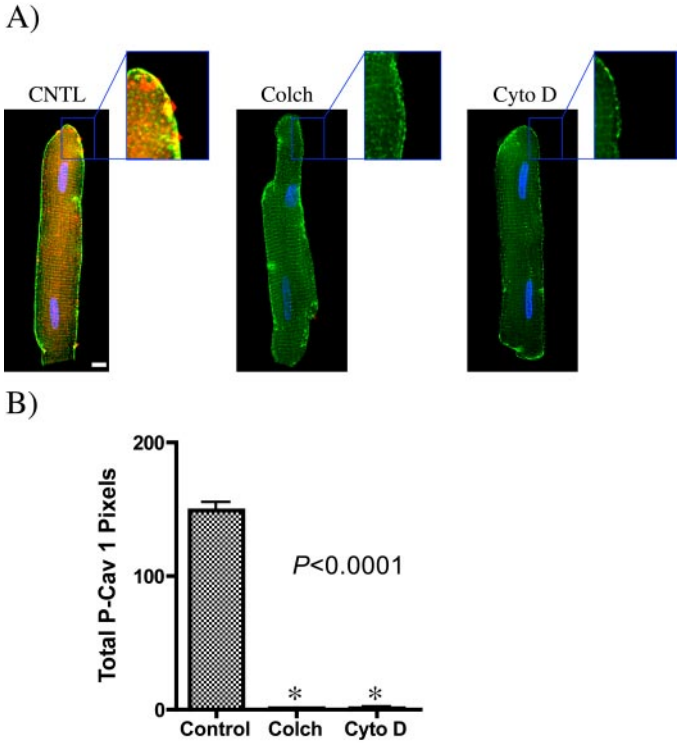

FIGURE 7. **Cytoskeletal disruption significantly decreases phosphocaveolin-1 (*P-Cav-1*) expression in cardiac myocytes.** *A*, immunofluorescence and deconvolution microscopy shows partial co-localization between P-Cav-1 (*red pixels*) and caveolin-3 (*green pixels*) on the sarcolemmal membrane and in sparse, intracellular locations. P-Cav-1 expression was significantly reduced ($p < 0.0001$) after treatment with Colch (30 μM; 1 h) and CD (*Cyto D*, 20 μM; 1.5 h). Incubation with secondary antibodies only shows minimal background staining (data not shown). *B*, quantitation of data were from experiments conducted on 3–5 cells isolated from three separate animals and is expressed as P-Cav-1 pixels. *Scale bar*, 10 μm. *CNTL*, control.

evidence that caveolin redistributes in aged and failing hearts (38) and that microtubules are disorganized in myotubes in caveolin-3 null mice (39).

Tissue remodeling involves alterations of both cellular and subcellular structures. For example, pressure-overload cardiac hypertrophy is associated with increased content of microtubules, whereas microtubular disruption increases contraction and alters Ca^{2+} currents, β-AR responsiveness, and heart rate in cardiac myocytes (40). Microtubular stabilization decreases cardiac Ca^{2+} transients, implying a role in regulation of calcium handling (41). In smooth muscle cells, increases in contractile tone due to mechanical stress result in cytoskeletal stiffening, actin accumulation at stress sites, and cell remodeling (42). Treatment of smooth muscle cells with cAMP or cytochalasin B causes disintegration of actin filaments (43), whereas treatment of endothelial cells with cAMP or agents that disrupt microtubules inhibits cell migration, and partial dissolution of microtubules leads to endothelial cell barrier dysfunction (44, 45). Thus, microtubules and actin filaments contribute to cell migration, cellular remodeling, and barrier function.

Despite the cytoskeletal inhibitor-promoted alterations in lipid rafts/caveolae and in localization of signaling components, we observed an enhancement in β-AR-stimulated cAMP production after treatment of CM with Colch,

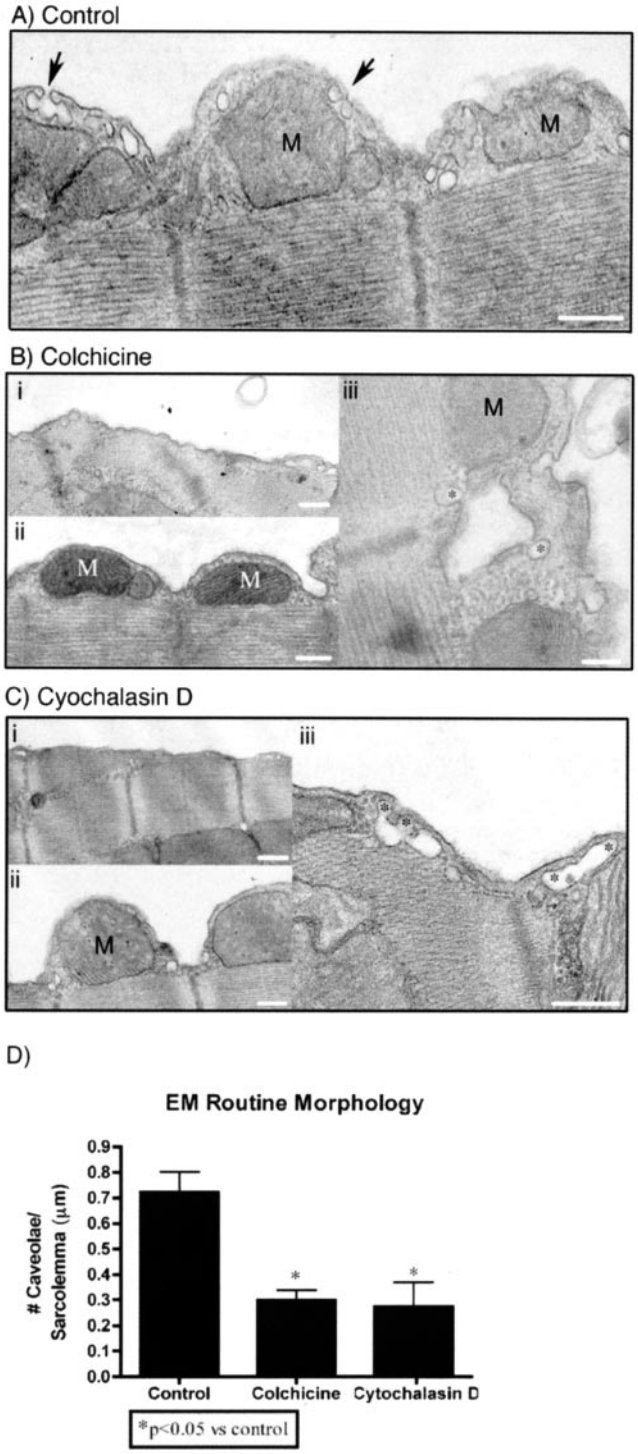

FIGURE 8. **Cytoskeletal disruption of adult cardiac myocytes decreases the number of sarcolemmal caveolae as determined by electron microscopy.** *A*, electron microscopic analysis demonstrates the presence of several caveolae (*arrows*) on the sarcolemmal membrane near subsarcolemmal mitochondria (*scale bar*, 1 μm). Colch (*B*) treatment significantly decreased ($p < 0.05$, $n = 3$) the number of total sarcolemmal caveolae. *Bi* and *Bii* (*scale bar*, 1 μm) show a decrease in the presence of caveolae while maintaining subsarcolemmal mitochondria and demonstrate the existence of vacuoles associated with Ω-shaped membranes (*asterisks*) (*Biii, scale bar* 0.2 μm) resembling caveolae. *Ci* and *Cii* demonstrate that cells treated with CD results in the loss of caveolae on the sarcolemma without displacing subsarcolemmal mitochondria (*scale bar*, 1 μm). *Ciii* (*scale bar* 0.5 μm) shows CD treatment results in clustering of structures resembling caveolae adjacent to the sarcolemma (*asterisks*). *D*, quantitation of data from three separate experiments is expressed as the number of caveolae/μm of sarcolemma. *M*, mitochondrion. *EM*, electron microscopy.

Downloaded from www.jbc.org at Biomedical Library, UCSD on April 15, 2009

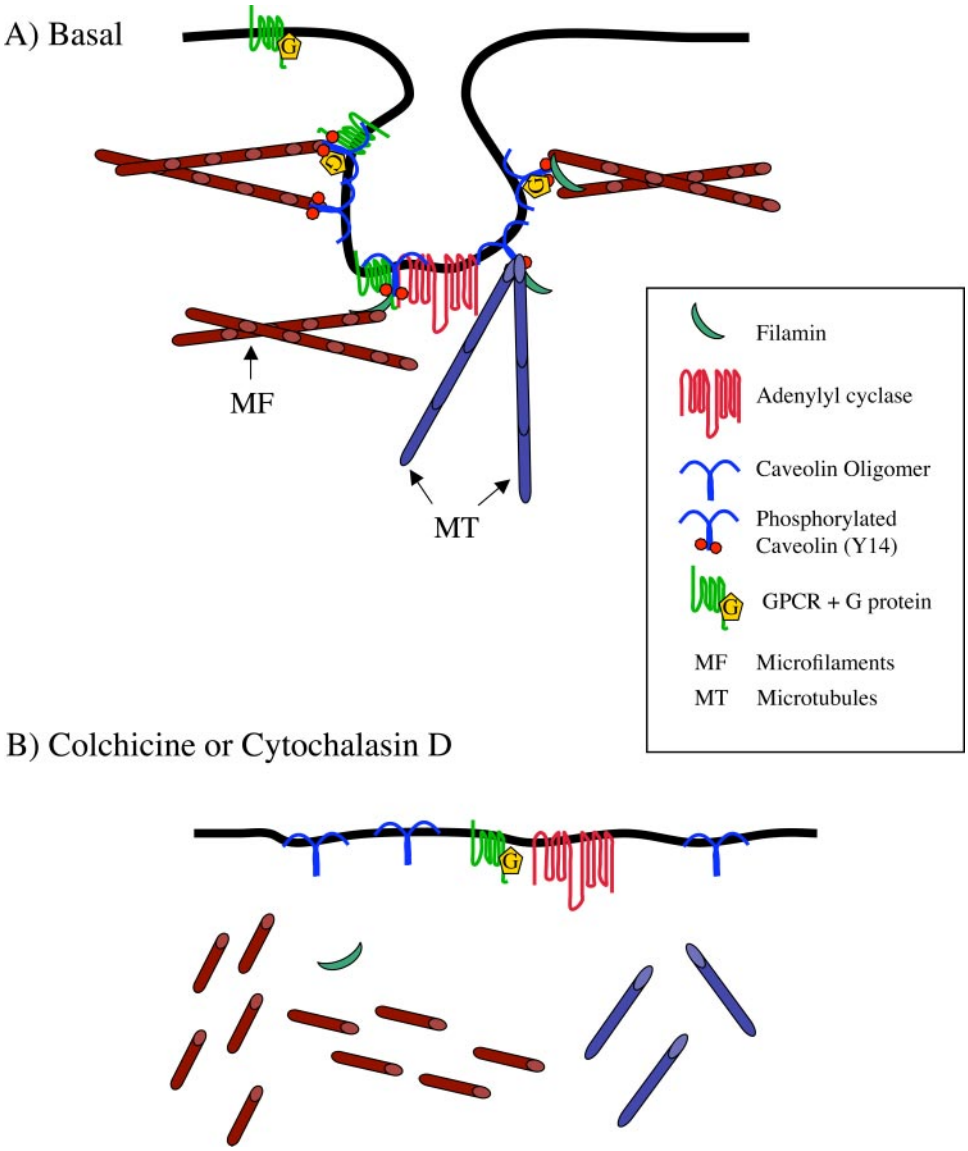

FIGURE 9. **Schematic diagram displaying the molecular organization of GPCR-associated signaling components in caveolar microdomains before (*A*) and after (*B*) cytoskeletal disruption.** *A*, under basal conditions, phosphorylated caveolin oligomers scaffold GPCRs, G proteins, and adenylyl cyclase within caveolar microdomains, and this depends upon intact cytoskeletal components. *B*, agents that disrupt microtubules (Colch) or actin filaments (CD) lead to the loss morphologic caveolae, decreased phosphorylation of caveolin oligomers, and a loss in the tonic inhibition of GPCR-mediated signal transduction by caveolin oligomers. The figure emphasizes caveolar domains but previous results and results shown in this manuscript imply that lipid rafts in cells without caveolae (*e.g.* S49 cells) can interact with cytoskeletal components and that in control cells this interaction restricts signal transduction by GPCR signaling components.

nocodazole, and CD (Fig. 1*D*); such results imply that caveolae-related GPCR-G_s-AC signal transduction is restrained by normal cytoskeletal assembly and dynamics. The findings in S49 cells imply that interaction of cytoskeletal components with lipid rafts even in the absence of caveolae restrain such interactions. The results provide a mechanism to explain findings in the numerous reports that have implicated cytoskeletal components in regulating cAMP synthesis and $[Ca]_i$ (6, 20, 21, 46) and may relate to the ability of microtubular depolymerization to increase $[Ca^{2+}]_i$ transients (47–49). Our results showing that cytoskeletal inhibitor-mediated loss of caveolae and redistribution of caveolin is associated with greater cAMP formation implies that an intact cytoskeleton acting via interaction with signaling components localized in lipid rafts and caveolae inhibits productive interaction among GPCR-G_s-AC (Fig. 9).

Tyrosine phosphorylation of caveolin has been associated with internalization of caveolae (4, 50). Cell detachment can produce a shift in localization of phosphocaveolin-1 from focal adhesion sites to caveolae and in the internalization of cholesterol-enriched membrane microdomains (50). We detected P-caveolin-1 and P-Src in buoyant fractions of CM, a co-localization that was lost after cytoskeletal disruption. Such findings implicate caveolar microdomains in maintenance of the fidelity of multiple signaling pathways and, in addition, as possible sites of attachment to the extracellular matrix in CMs and perhaps other cells (51).

We also found constitutive phosphorylation of caveolin-1, caveolin-2, p38 MAPK, and Src in CMs but that such phosphorylation was reduced after treatment with agents that decrease the presence of caveolae (Figs. 4 and 8). Although the role of phosphorylated caveolins in signal transduction is not well understood, we hypothesize that such phosphorylation is important for maintaining caveolin hetero- and homo-oligomers (29, 52) and for scaffolding and recruitment of signaling components (53, 54) to caveolin-associated complexes, perhaps by stabilizing multiprotein complexes between caveolar resident and cytoskeletal proteins (*i.e.* tubulin and filamin), thereby optimizing cell signaling. In this regard, it is of note that in hypertrophied hearts, one finds a transient increase in the number of caveolae and abnormal caveolae associated with filamentous structures (37) and an increase in phosphorylated Src tyrosine kinase at Tyr-416 (55), the site required for caveolin phosphorylation. Such results suggest that cytoskeleton-membrane junctions may contain binding domains for Src family kinases and that phosphorylation by these kinases is important for signal transduction (56). Because low M_r phosphotyrosine-protein phosphatase and protein-tyrosine phosphatase 1B localize to caveolae, co-immunoprecipitate with caveolin (51), and dephosphorylate P-Cav (31, 57), future studies that assess the impact of cytoskel-

Downloaded from www.jbc.org at Biomedical Library, UCSD on April 15, 2009

etal disruption on distribution and activity of these enzymes should prove of interest.

In conclusion, disruption of microtubules and the actin cytoskeleton produces loss of morphologic caveolae and redistribution of caveolar/lipid raft-resident proteins in parallel with increases in cAMP production, results that help explain previous observations related to the ability of cytoskeletal inhibitors to increase cellular cAMP levels. The ability of cytoskeletal components to influence caveolar-resident protein interactions and the phosphorylation state of caveolins has implications for signal transduction processes as well as for age- and pathophysiological-related changes in the heart and other tissues (38).

Acknowledgments—We are grateful for the technical assistance from the University of California San Diego Cancer Center Digital Imaging Shared Resource, in particular Jim Feramisco and Steve McMullen. In some cases, three-dimensional perspective views were made at the VisLab in the San Diego Supercomputer Center using NPACI Scalable Visualization Tools.

REFERENCES

1. Chang, L., and Goldman, R. D. (2004) *Nat. Rev. Mol. Cell Biol.* **5,** 601–613
2. Gundersen, G. G. (2002) *Nat. Rev. Mol. Cell Biol.* **3,** 296–304
3. Revenu, C., Athman, R., Robine, S., and Louvard, D. (2004) *Nat. Rev. Mol. Cell Biol.* **5,** 635–646
4. Pelkmans, L., Puntener, D., and Helenius, A. (2002) *Science* **296,** 535–539
5. Mundy, D. I., Machleidt, T., Ying, Y. S., Anderson, R. G., and Bloom, G. S. (2002) *J. Cell Sci.* **115,** 4327–4339
6. Insel, P. A., and Kennedy, M. S. (1978) *Nature* **273,** 471–473
7. Kennedy, M. S., and Insel, P. A. (1979) *Mol. Pharmacol.* **16,** 215–223
8. Leiber, D., Jasper, J. R., Alousi, A. A., Martin, J., Bernstein, D., and Insel, P. A. (1993) *J. Biol. Chem.* **268,** 3833–3837
9. Jasper, J. R., Post, S. R., Desai, K. H., Insel, P. A., and Bernstein, D. (1995) *J. Pharmacol. Exp. Ther.* **274,** 937–942
10. Stahlhut, M., and van Deurs, B. (2000) *Mol. Biol. Cell* **11,** 325–337
11. Palade, G. (1953) *J. Appl. Physiol.* **24,** 1424–1436
12. Pike, L. J. (2003) *J. Lipid Res.* **44,** 655–667
13. Thomsen, P., Roepstorff, K., Stahlhut, M., and van Deurs, B. (2002) *Mol. Biol. Cell* **13,** 238–250
14. Parton, R. G., and Richards, A. A. (2003) *Traffic* **4,** 724–738
15. Isshiki, M., and Anderson, R. G. (2003) *Traffic* **4,** 717–723
16. Parton, R. G., Way, M., Zorzi, N., and Stang, E. (1997) *J. Cell Biol.* **136,** 137–154
17. Steinberg, S. F., and Brunton, L. L. (2001) *Annu. Rev. Pharmacol. Toxicol.* **41,** 751–773
18. Head, B. P., Patel, H. H., Roth, D. M., Lai, N. C., Niesman, I. R., Farquhar, M. G., and Insel, P. A. (2005) *J. Biol. Chem.* **280,** 31036–31044
19. van der Heyden, M. A., Wijnhoven, T. J., and Opthof, T. (2005) *Cardiovasc. Res.* **65,** 28–39
20. Rasenick, M. M., Stein, P. J., and Bitensky, M. W. (1981) *Nature* **294,** 560–562
21. Donati, R. J., and Rasenick, M. M. (2005) *Neuropsychopharmacology* **30,** 1238–1245
22. Ostrom, R. S., Liu, X., Head, B. P., Gregorian, C., Seasholtz, T. M., and Insel, P. A. (2002) *Mol. Pharmacol.* **62,** 983–992
23. Song, K. S., Li, S., Okamoto, T., Quilliam, L. A., Sargiacomo, M., and Lisanti, M. P. (1996) *J. Biol. Chem.* **271,** 9690–9697
24. Zinchuk, O., Fukushima, A., and Hangstefer, E. (2004) *Cell Tissue Res.* **317,** 265–277
25. De Vries, L., Elenko, E., McCaffery, J. M., Fischer, T., Hubler, L., McQuistan, T., Watson, N., and Farquhar, M. G. (1998) *Mol. Biol. Cell* **9,** 1123–1134
26. Goldman, R. D. (1971) *J. Cell Biol.* **51,** 752–762
27. Mons, S., Veretout, F., Carlier, M., Erk, I., Lepault, J., Trudel, E., Salesse, C., Ducray, P., Mioskowski, C., and Lebeau, L. (2000) *Biochim. Biophys. Acta* **1468,** 381–395
28. van Deurs, B., von Bulow, F., Vilhardt, F., Holm, P. K., and Sandvig, K. (1996) *J. Cell Sci.* **109,** 1655–1665
29. Capozza, F., Cohen, A. W., Cheung, M. W., Sotgia, F., Schubert, W., Battista, M., Lee, H., Frank, P. G., and Lisanti, M. P. (2005) *Am. J. Physiol. Cell Physiol.* **288,** 677–691
30. Halayko, A. J., and Stelmack, G. L. (2005) *Can. J. Physiol. Pharmacol.* **83,** 877–891
31. Lee, H., Xie, L., Luo, Y., Lee, S. Y., Lawrence, D. S., Wang, X. B., Sotgia, F., Lisanti, M. P., and Zhang, Z. Y. (2006) *Biochemistry* **45,** 234–240
32. Thomas, S., Preda-Pais, A., Casares, S., and Brumeanu, T. D. (2004) *Mol. Immunol.* **41,** 399–409
33. Huang, C., Hepler, J. R., Chen, L. T., Gilman, A. G., Anderson, R. G., and Mumby, S. M. (1997) *Mol. Biol. Cell* **8,** 2365–2378
34. Volonte, D., Galbiati, F., Pestell, R. G., and Lisanti, M. P. (2001) *J. Biol. Chem.* **276,** 8094–8103
35. Tsutsui, H., Ishihara, K., and Cooper, G. (1993) *Science* **260,** 682–687
36. Zile, M. R., Green, G. R., Schuyler, G. T., Aurigemma, G. P., Miller, D. C., and Cooper, G. (2001) *J. Am. Coll. Cardiol.* **37,** 1080–1084
37. Goto, Y., Yoshikane, H., Honda, M., Morioka, S., Yamori, Y., and Moriyama, K. (1990) *J. Submicrosc. Cytol. Pathol.* **22,** 535–542
38. Ratajczak, P., Damy, T., Heymes, C., Oliviero, P., Marotte, F., Robidel, E., Sercombe, R., Boczkowski, J., Rappaport, L., and Samuel, J. L. (2003) *Cardiovasc. Res.* **57,** 358–369
39. Volonte, D., Peoples, A. J., and Galbiati, F. (2003) *Mol. Biol. Cell.* **14,** 4075–4088
40. Tagawa, H., Koide, M., Sato, H., Zile, M. R., Carabello, B. A., and Cooper, G. (1998) *Circ. Res.* **82,** 751–761
41. Howarth, F. C., Calaghan, S. C., Boyett, M. R., and White, E. (1999) *J. Physiol.* (*Lond.*) **516,** 409–419
42. Deng, L., Fairbank, N. J., Cole, D. J., Fredberg, J. J., and Maksym, G. N. (2005) *J. Appl. Physiol.* **99,** 634–641
43. Chaldakov, G. N., Nabika, T., Nara, Y., and Yamori, Y. (1989) *Cell Tissue Res.* **255,** 435–442
44. Naito, M., Hayashi, T., Kuzuya, M., Funaki, C., Asai, K., and Kuzuya, F. (1989) *Artery* **17,** 21–31
45. Birukova, A. A., Birukov, K. G., Adyshev, D., Usatyuk, P., Natarajan, V., Garcia, J. G., and Verin, A. D. (2005) *J. Cell. Physiol.* **204,** 934–947
46. Zor, U. (1983) *Endocr. Rev.* **4,** 1–21
47. Galli, A., and DeFelice, L. J. (1994) *Biophys. J.* **67,** 2296–2304
48. Kolodney, M. S., and Elson, E. L. (1995) *Proc. Natl. Acad. Sci. U. S. A.* **92,** 10252–10256
49. Webster, D. R., and Patrick, D. L. (2000) *Am. J. Physiol. Heart Circ. Physiol.* **278,** 1653–1661
50. del Pozo, M. A., Balasubramanian, N., Alderson, N. B., Kiosses, W. B., Grande-Garcia, A., Anderson, R. G., and Schwartz, M. A. (2005) *Nat. Cell Biol.* **7,** 901–908
51. Swaney, J. S., Patel, H. H., Yokoyama, U., Head, B. P., Roth, D. M., and Insel, P. A. (2006) *J. Biol. Chem.* **281,** 17173–17179
52. Lee, H., Park, D. S., Wang, X. B., Scherer, P. E., Schwartz, P. E., and Lisanti, M. P. (2002) *J. Biol. Chem.* **277,** 34556–34567
53. Cao, H., Courchesne, W. E., and Mastick, C. C. (2002) *J. Biol. Chem.* **277,** 8771–8774
54. Cao, H., Sanguinetti, A. R., and Mastick, C. C. (2004) *Exp. Cell Res.* **294,** 159–171
55. Kuppuswamy, D., Kerr, C., Narishige, T., Kasi, V. S., Menick, D. R., and Cooper, G. (1997) *J. Biol. Chem.* **272,** 4500–4508
56. Fox, J. E., Lipfert, L., Clark, E. A., Reynolds, C. C., Austin, C. D., and Brugge, J. S. (1993) *J. Biol. Chem.* **268,** 25973–25984
57. Caselli, A., Taddei, M. L., Manao, G., Camici, G., and Ramponi, G. (2001) *J. Biol. Chem.* **276,** 18849–18854

Downloaded from www.jbc.org at Biomedical Library, UCSD on April 15, 2009